divided by the separation time between adjacent echo reflections. The reflected echo separation times were determined to be 1.64 μs to give a speed of sound for a compressional wave in glaze ice of 3.94 mm/μs. This compares favorably with the results obtained in Ref. 7. The time separation between echoes 1 and 9 was 9.72 μs and corresponds to the travel time of the compressional wave through the front piece of aluminum and the ice trough. In Fig. 3, results are shown that give multiple echoes for shear waves coupled into the ice. The time difference between echoes 1 and 2, 2 and 3, 4 and 5, 5 and 6, represents how long it took for the shear wave to travel through the ice. The time was determined to be 3.25 μs. For a trough width of 3.23 mm, this gave a shear sound speed of 1.99 mm/μs in ice. This measurement gives a shear sound speed in ice of approximately one-half that for a compressional wave.

Concluding Remarks

Data are given to show how sound-speed measurements in refrigerated ice were determined using both compressional and shear waves. Oscilloscope traces were obtained using pulse-echo ultrasonics experimental procedures. Two parameters were needed to determine sound speeds in ice using this technique. These parameters were the ice thickness and the time of travel of the sound wave through ice. The time measurements were obtained from an oscilloscope trace using time cursor markers with trace overlapping ability and digital time readout on the oscilloscope screen. The ice thickness was forced to be a known value by machining a trough in an aluminum block. All surfaces of the aluminum blocks coming in contact with the sound beam were machined to a smooth 32 microfinish to assure good transmission and reflection of the sound waves at the aluminum interfaces. Clear and sharp echo reflections were obtained for both compressional and shear waves at the aluminum/ice and ice/aluminum interfaces. The geometry chosen permits accurate determination of sound speeds in ice through the use of a known ice thickness and smooth surfaces in the sound beam path. Typically, the top surface of ice formed while exposed to air will not be smooth and flat. This can contribute to mode conversions and other echo reflcetion variations. The type of geometry and surface preparation chosen ensures that the ice surfaces interacting with the sound beam will be bonded to a smooth surface.

The work presented in this report was done at one ice temperature. It is recognized that the properties of ice can vary, depending on certain environmental conditions. Ice formed at various conditions can have different sound speeds depending on the density and elastic constants. The sound speeds in ice reported here are expected to be good for the conditions given: refrigerated ice at $-26°C$.

References

[1]Ponder, E.R., *The Physics of Ice,* Pergamon Press, Elmsford, NY, 1965, pp. 107-115.

[2]Filipczynski, L., Pawlowski, Z., and Wehr, J. Jr., *Ultrasonic Methods of Testing Materials,* Butterworth, London, 1966, pp. 12-15.

[3]Jeck, R.K., "A New Data Base of Supercooled Cloud Variables for Altitudes up to 10,000 Feet AGL and the Implications for Low Altitude Aircraft Icing," NRL Report 8738, Aug. 1983.

[4]Masters, C.O., "A New Characterization of Supercooled Clouds Below 10,000 Feet AGL," Rept. DOT/FAA/CT-83/22, June 1983.

[5]Flight Safety Research Branch, ACT-340, "Engineering and Development Program Plan-Aircraft Icing," Rept. DOT/FAA/CT-83/7, Aug. 1983.

[6]Magenheim, B. and Rocks, J.K., "Developement and Test of a Microwave Ice Accretion Measurement Instrument (MIAMI)," NASA CR-3598, 1982.

[7]Hansman, R.J. Jr. and Kirby, M.S., "Measurements of Ice Accretion Using Ultrasonic Pulse-Echo Techniques," *Journal of Aircraft,* Vol. 22, June 1985, PP. 530-535.

Noninvasive Experimental Technique for the Measurement of Unsteady Velocity Fields

L. Lourenco* and A. Krothapalli†
Florida State University, Tallahassee, Florida
and
J.M. Buchlin‡ and M.L. Riethmuller‡
von Kármán Institute for Fluid Dynamics
Rhode-St-Genese, Belgium

Introduction

ONE of the difficult problems in experimental fluid mechanics remains the measurement of velocity and vorticity fields in unsteady flows. Current methods for the measurement of vorticity involve the use of multiple hot-wire anemometers or laser Doppler velocimeters to independently measure the components of the velocity vector at closely spaced locations. The "local" flow vorticity is then determined by applying a finite-difference scheme to the measured velocity components. However, these techniques suffer from some drawbacks. First, the presence of several hot-wire probes in a small region of the flow produces significant blockage effects that perturb the local flow pattern. Second, in most cases, the distance between the multiple measuring volumes is not small enough to accurately resolve the local velocity gradients. This results in "spatially filtered" vorticity estimates. Third, these methods can provide only "one-point" information. In order to obtain data on the entire field, measurements must be carried out sequentially one point at a time. Although this sequential procedure can be easily implemented to investigate steady flows, it is rather difficult to use in unsteady flows.

When a global and instantaneous picture of the flowfield is required, researchers rely heavily on various flow visualization techniques. Traditionally, flow visualization pictures have been used to qualitatively study global flow properties. However, with the advent of fast computers, capable of handling high-resolution images, it is now possible to combine advanced visualization techniques with digital processing algorithms to obtain quantitative information.

This note presents a new technique known as particle image displacement velocimetry, which permits the visualization of two-dimensional flows as well as the quantification of the instantaneous velocity and vorticity fields.

Principle of the Technique

The principle of operation of particle image displacement velocimetry (PIDV) is sketched on Fig. 1. It involves two equally important steps. In the first step, a plane of the flow seeded with small particles is recorded (Fig. 1a). A sheet of light produced by a laser source illuminates a selected plane of the flow. A pulsed laser, such as a ruby or a NdYag laser, or a continuous wave (CW) laser with a shutter device, is used as the light source. The light scattered by the seeding particles in the illuminated plane provides a moving pattern. For low seeding concentrations, this pattern consists of resolved dif-

Received Nov. 12, 1985; revision received Jan. 24, 1986.

*Assistant Professor of Mechanical Engineering, FAMU/FSU College of Engineering. Member AIAA.
†Associate Professor of Mechanical Engineering, FAMU/FSU College of Engineering. Member AIAA.
‡Associate Professor.

fraction limited images of the particles.[1] A multiple-exposure photograph records this moving pattern. In a second step, the flow visualization photograph is analyzed. The local fluid velocity is derived from the ratio between the measured spacing between consecutive images of the same particle and the time between exposures. This is accomplished using an interferometric method (Fig. 1b). The diffraction produced by local coherent illumination of the multiple images of the particles generates straight Young's fringes in the Fourier plane of a lens. These fringes have an orientation perpendicular to the direction of the local displacement vector and a spacing inversely proportional to its magnitude.

Except for some subtle differences in the first step (see Ref. 2 for more details), a similar technique known as laser speckle velocity was first successfully applied to the problem of transient Bénard convection by Simpkins and Dudderar.[3] Using the same technique, Meynart[4] made measurements in a low Reynolds number axisymmetric jet. Although good definition of the velocity field was obtained within the potential core region of the jet, due to the limited velocity range, the full vortical regions were not captured. The focus of this Note is to show the application of PIDV to an aerodynamic flow dominated by vortical motions. Unlike in the previous applications of a similar technique, this Note also presents a successful use of a low-power CW laser to record the unsteady vorticle flowfield.

Validation of the Technique

Experimental Configuration

The capabilities of the present technique are evaluated in a measurement of the flow past an impulsively started NACA 0012 airfoil at 30 deg incidence. The flow is created by towing a 60 mm chord airfoil (span = 240 mm) at a constant velocity of 23.5 mm/s in a tank (300 × 300 × 600 mm) filled with water. A detailed examination showed that the motion of the towing carriage is smooth and vibration free. The water is seeded with small (4 μm in diameter) particles (TSI model 10087). The corresponding flow Reynolds number is 1400. A laser sheet 70 mm wide and 0.3 mm thick, produced from a 5 W argon ion laser illuminates the midspan section of the model. For the multiple exposure, the CW laser beam is modulated using a Bragg cell.[5] The power density of the laser sheet is $I_0 = 0.27$ W/mm^2.

A 100 × 127 mm format camera with a 135 mm focal length lens is used for the photographic recording. The lens aperture is f5.6 and the magnification factor M is 0.47. The camera was positioned in the laboratory reference frame, which means that our observation point is fixed in relation to the fluid. The film used is a Kodak technical pan 2415, preflashed to achieve increased sensitivity and overexposed for better contrast.

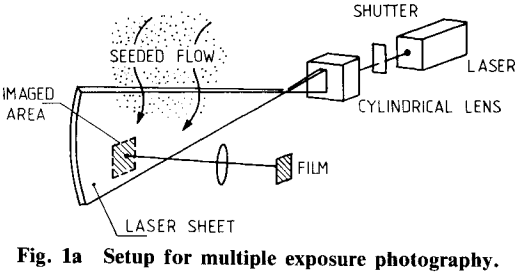

Fig. 1a Setup for multiple exposure photography.

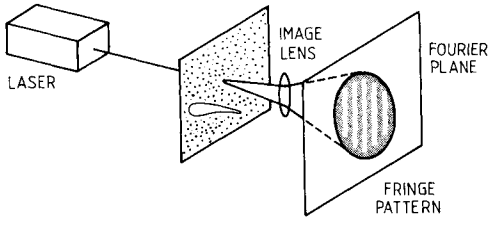

Fig. 1b Setup for the generation of young's fringes.

For the multiple exposure, the time between exposures T and the exposure time t are chosen according to the criteria discussed in Ref. 1 and are, respectively,

$$T = 0.5D/MV_{\max} = 11\text{ms} \tag{1}$$

$$t = d_i/MV_{\max} = 1\text{ms} \tag{2}$$

where D is the analyzing beam diameter, $V_{\max}$ the maximum expected velocity in the field, and d_i the particle image diameter expressed in terms of

$$d_i = (d_p^2 + d_s^2)^{1/2} \tag{3}$$

with d_p the particle diameter and d_s the edge spread caused by the limited response of the recording optics.[6] The exposure time and the time between exposures together with the particle image size diameter determine the technique's velocity dynamic range V, defined as the largest velocity difference that can be detected in the flowfield as

$$V = \frac{V_{\max} - V_{\min}}{V_{\min}} = \frac{D - 2d_i}{2Md_i} - 1 \simeq 6 \tag{4}$$

Results

Figure 2 is a triple exposure photograph of the flow past an impulsively started airfoil. In this photograph, the flow is captured at a stage of its development corresponding to $t^* = tU/C = 2$, the nondimensional time, where t is the time from startup, U the freestream velocity and C the airfoil chord length. The velocity data are acquired in a regular mesh by digital processing of the Young's fringes, produced by point-by-point scanning of the photograph. The scanning step size and the dimension of the analyzing beam diameter are 0.5 mm, which corresponds to a spatial resolution of about 1 mm of the actual flowfield. This spacing proves to be small enough to accurately estimate the vorticity. However, if required, smaller scanning step sizes can be used. The fringe patterns were processed using the interactive one-dimensional averaging software described in Refs. 4 and 6. Figure 3 displays the mapped two-dimensional velocity vector field. Because the two-dimensional velocity field is acquired on a square mesh, the spatial derivatives of the velocity and, consequently, the vorticity can be estimated by a simple algorithm. Considering that the grid locations of the measurement points are labeled with indices i, j, the vorticity component $\Omega_{i,j}$ at location i,j is

$$\Omega_{i,j} = \frac{1}{2}\left[\frac{V_{i+1,j} - V_{i-1,j}}{2\Delta x} - \frac{U_{i,j+1} - U_{i,j-1}}{2\Delta y}\right]$$

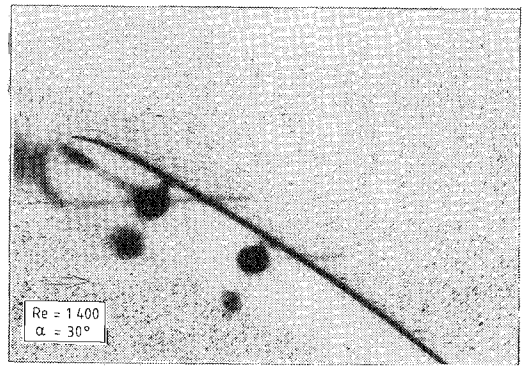

Fig. 2 Triple-exposed photograph of the flow over a NACA 0012 airfoil.

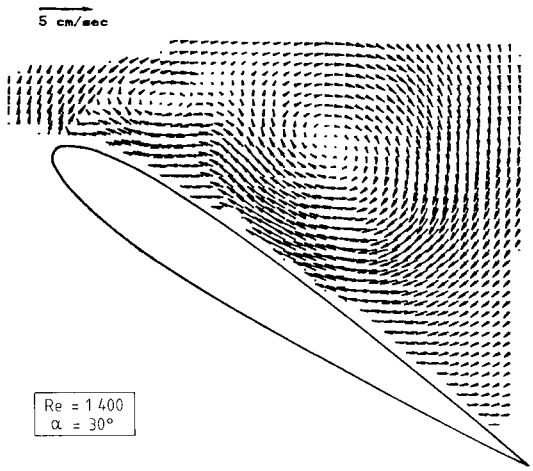

Fig. 3 Instantaneous velocity field over a NACA 0012 airfoil.

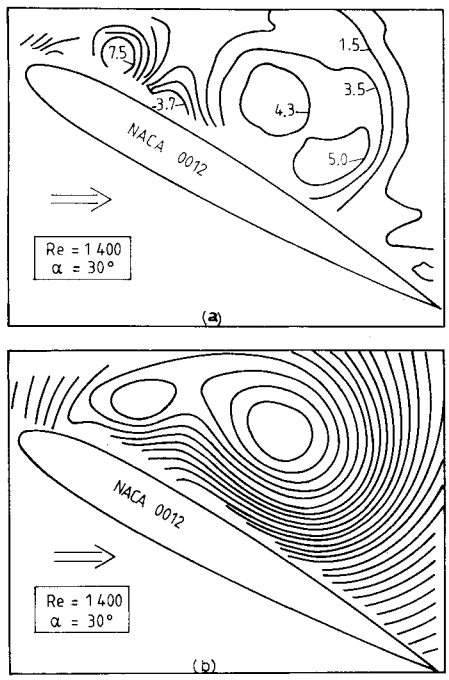

Fig. 4 Flow over NACA 0012 airfoil: a) isovorticity contours, b) streamline pattern.

For the boundaries of the velocity field, an excentered scheme is used to evaluate the spatial derivatives. Figure 4a displays the vorticity contours. An improved representation of the flowfield is obtained using the stream function (Fig. 4b). The later is computed using the vorticity values and integrating the Poisson equation. The features of this flowfield, for the Reynolds number presented here and for angles of attack greater than 15 deg, can be described as follows. First, a starting vortex is created at the trailing edge and sheds immediately downstream. This process occurs for $t^* < 0.1$. Concomitant with this, the flow at the leading edge separates and forms a closed recirculating bubble. This bubble is then convected downstream (large vortex in Fig. 3) as a vortex along the upper surface of the airfoil. This vortex is accompanied on its upstream side by another small vortex, as shown in Fig. 3. Similar observations were made by other investigators using conventional visualization techniques. However, Figs. 3 and 4 show vividly the quantitative velocity field and associated vorticity, along with a clear definition of the location of the vortex centers, vortex size, and the flow separation and reattachment points.

Conclusion

Particle image displacement velocimetry is a cost effective way to provide both quantitative and qualitative information of two-dimensional flowfields. This method is well suited to evaluate the velocity and vorticity distribution in unsteady flows and the data obtained may be used to gather both temporal and spatial information. Therefore, it is expected that this technique will permit a more detailed study of complex flowfields.

References

[1]Lourenco, L.M. and Krothapalli, A., "The Role of Photographic Parameters in Laser Speckle or Particle Image Displacement Velocimetry," *Experiments in Fluids*, to be published.

[2]Lourenco, L.M. and Krothapalli, A., "The Development of Laser Speckle or Particle Image Displacement Velocimetry, Part 1: The Role of Photographic Parameters," Florida State University, Tallahassee, Rept. FMRL-TR-1, 1985.

[3]Simpkins, P.G. and Dudderar, T.D., "Laser Speckle Measurements of Transient Bénard Convection," *Journal of Fluid Mechanics*, Vol. 89, 1978, pp. 665-671.

[4]Meynart, R., "Speckle Velocimetry Study of a Vortex Pairing in a Low Re Number Unexited Jet," *The Physics of Fluids*, Vol. 26, 1983, pp. 2077-2079.

[5]Lourenco, L.M. and Whiffen, M.C., "Laser Speckle Methods in Fluid Dynamics Applications," Paper presented at International Symposium on Application of Laser Velocimetry to Fluid Mechanics, Lisbon, 1984.

[6]Adrian, R.J. and Yao, C.S., "Development of Pulsed Laser Velocimetry for the Measurement of Fluid Flow," *Proceedings of Eighth Biennial Symposium on Turbulence*, Rolla, MO, 1984.

Multiple-Scale Turbulence Model in Confined Swirling Jet Predictions

C. P. Chen*
NASA Marshall Space Flight Center
Huntsville, Alabama

Introduction

In the last decade, advances have been made in turbulence modeling such that it is now possible to predict mean and turbulence characteristics of many shear flows. Among the models, the so called k-ϵ model has been shown to be adequate in a variety of flows.[1] However, in complex flows, such as confined swirling flows, the k-ϵ model is known to be deficient[2] due to the neglect of anisotropy in the turbulent viscosity and additional turbulence generation arising from streamline curvature. Several recent proposals,[3,4] which modify the k-ϵ model based on the streamline curvature Richardson numbers, give improved predictions in only certain limited regions of the swirling flow.[5,6] The purpose of this Note is to present a recently developed multiple-scale turbulence model, which seeks to circumvent deficiencies of earlier models by taking into account the nonequilibrium spectral energy transfer. The validity of this model is tested by predicting the confined swirling coaxial jet flow in a sudden expansion.

Received Oct. 25, 1985; revision received March 3, 1986.

*NRC-NASA Research Associate, Fluid Dynamics Branch, System Dynamics Laboratory.